Am J Physiol Gastrointest Liver Physiol 294: G627–G634, 2008.
First published December 20, 2007; doi:10.1152/ajpgi.00519.2007.

Active and inactive pools of nNOS in the nerve terminals in mouse gut: implications for nitrergic neurotransmission

Y. Manjula Rao, Arun Chaudhury, and Raj K. Goyal

Center for Swallowing and Motility Disorders, Veterans Affairs Boston Healthcare System and Harvard Medical School, Boston, Massachusetts

Submitted 9 November 2007; accepted in final form 19 December 2007

Rao YM, Chaudhury A, Goyal RK. Active and inactive pools of nNOS in the nerve terminals in mouse gut: implications for nitrergic neurotransmission. *Am J Physiol Gastrointest Liver Physiol* 294: G627–G634, 2008. First published December 20, 2007; doi:10.1152/ajpgi.00519.2007.—Nitric oxide (NO) is responsible for nitrergic neurotransmission in the gut, and its release is dependent on its de novo synthesis by neuronal nitric oxide synthase (nNOS). The magnitude of NO synthesis and release during neurotransmission may be related to the fraction of catalytically active nNOS out of a larger pool of inactive nNOS in the nerve terminals. The purpose of the present study was to identify catalytically active and inactive pools of nNOS in the varicosities from mouse gut. Enteric varicosities were confirmed as nitrergic by colocalization of nNOS with the nerve varicosity marker synaptophysin. Low-temperature SDS-PAGE of these varicosity extracts showed 320-, 250-, and 155-kDa bands when blotted with anti-nNOS$_{1422–1433}$ and 320- and 155-kDa bands when blotted with anti-nNOS$_{1–20}$ antibodies, respectively. The 320- and 155-kDa bands represent dimers and monomers of nNOSα; the 250- and 135-kDa bands represent dimers and monomers of nNOSβ. Immunoprecipitation with calmodulin (CaM) showed that a portion of nNOSα dimer was bound with CaM. On the other hand, a portion of nNOSα dimer, nNOSβ dimer, and all monomers lacked CaM binding. The CaM-lacking nNOS fractions reacted with anti-serine 847-phospho-nNOS. In vitro assays of NO production revealed that only the CaM-bound dimeric nNOSα was catalytically active; all other forms were inactive. We suggest that the amount of catalytically active nNOSα dimers may be regulated by serine 847 phosphorylation and equilibrium between dimers and monomers of nNOSα.

nitric oxide; isoforms of nNOS; serine 847-phosphorylated nNOS; enteric nerve varicosities; calmodulin-bound nNOS

NITRIC OXIDE (NO) generated by neuronal nitric oxide synthase (nNOS) is responsible for nitrergic inhibitory neurotransmission in the gut (4, 15, 25). However, regulation of nitrergic neurotransmission is not well understood. The classical neurotransmitters, acetylcholine and catecholamines, are preformed and stored in secretory granules in the nerve terminals. The secretory granules exist as a large "reserve" pool and a smaller "readily releasable" pool; the latter is docked on the varicosity membrane. During nerve stimulation, propagation of an action potential in the nerve terminal causes influx of calcium into the terminal, resulting in a quantal release of the transmitter from the releasable pool (21). Regulation of the readily releasable pool of the secretory granules serves as an important determinant of the amount of the neurotransmitters released with each episode of nerve stimulation. On the other hand, NO is a highly diffusible gas and it is not preformed nor stored in secretory granules. nNOS localized to membranes of neural dendrites and motor nerve terminals are the tentative sites of NO generation during retrograde and anterograde nitrergic neurotransmission, respectively (5, 11). It is possible that only a specific fraction of nNOS in the nerve terminal with catalytic activity participates in NO production by the action of calcium influx upon nerve stimulation. We hypothesized that, analogous to the control of the amount of release of the classical neurotransmitters, NO synthesis and release may be regulated by the pools of catalytically active and inactive forms of nNOS in the varicosities. However, the nature of these catalytically active and inactive nNOS pools in the nerve terminals is not well known.

Studies have shown that the catalytically active nNOS is a tetramer of two molecules of nNOS associated with two molecules of calmodulin (CaM) (2, 18, 24). In addition, targeting of nNOS to the nerve terminal is also critical in neurotransmission. Some nNOS isoforms possess PDZ binding domains. PDZ is an acronym for postsynaptic density protein (PSD95), *Drosophila* disc large tumor suppressor (DlgA), and zonula occludens-1 protein (ZO-1). PSD95 is anchored to specific regions of the cell membrane. Therefore, protein-protein interactions involving PDZ binding domains allow anchoring of nNOS to the cell membrane via PSD95. Studies in hippocampal neurons have shown that the isoforms of nNOS possessing PDZ binding domains are targeted to the complementary PDZ binding domain-containing PSD95 in the dendrites of the hippocampal neurons (19). Similarly, it is possible that PDZ domain-containing nNOS isoforms are targeted to the motor nerve terminals in the gut. Thus, CaM-binding and dimerization of nNOS isoform containing PDZ binding domain may constitute the active nNOS that produces NO from L-arginine during calcium influx caused by action potentials invading the nitrergic nerve terminals (6, 12, 18).

The purpose of the present study was to identify catalytically active and inactive pools of nNOS in varicosities obtained from mouse gut. Immunoblots, immunoprecipitation, and functional assays were performed to identify *1*) splice variants of nNOS; *2*) dimers and monomers in the native extract; *3*) CaM-bound and CaM-lacking nNOS fractions; *4*) the nature of the CaM-lacking nNOS isoforms; and *5*) nNOS fractions that were catalytically active and produced NO in an in vitro assay system.

MATERIALS AND METHODS

The experimental protocols used in this study were approved by the Institutional Animal Care and Use Committee of Veterans Affairs Boston Healthcare System.

Address for reprint requests and other correspondence: R. K. Goyal, VA Medical Center, 1400 VFW Parkway, West Roxbury, MA 02132 (e-mail: raj_goyal@hms.harvard.edu).

The costs of publication of this article were defrayed in part by the payment of page charges. The article must therefore be hereby marked "*advertisement*" in accordance with 18 U.S.C. Section 1734 solely to indicate this fact.

Antibodies and chemicals. Details of all the antibodies used in the present study are summarized in Table 1. The anti-serine 847-phospho-nNOS antibody was raised against 848KRFNSVS854 of human nNOS that recognized serine 852 phosphorylation in the human sequence and corresponded with the sequence 844RFNSVS849 in the mouse nNOS (Santa Cruz). Thus, in mice, this antibody recognizes the serine 847-phosphorylated nNOS. All secondary antibodies were obtained from Jackson Immunochemicals and Santa Cruz. Reagents for immunoblot and chemicals used were from Bio-Rad, Wako Chemicals, and Sigma. Immunoprecipitation reagents (Protein A/G) were from Roche Molecular Biochemicals and Santa Cruz.

Tissue dissection. Adult male C57BL/6j mice (25–30 g each) (Jackson Laboratories) were euthanized by carbon dioxide (CO_2) inhalation in an airtight chamber. Gastrointestinal tissues from three to six mice were pooled for each experiment. For protein interaction studies, six to ten mice were used for preparing each varicosity extract to ensure abundance of proteins of interest. The entire gastrointestinal tract from the stomach to colon was dissected quickly and opened along the antimesenteric border. The gut lumen was cleaned in ice-cold homogenization buffer (0.3 M sucrose with 0.1 M sodium phosphate and 1 mM EGTA, pH 7.4). Small pieces of intestine were placed in a plastic tube in 10 volumes of the homogenization buffer described earlier and were pulverized into a homogenous extract with a Brinkmann homogenizer, and the tube was cooled on ice before further processing. The homogenization buffers contained adequate quantities of protease and phosphatase inhibitors. [The protease inhibitor was used at a concentration of 1 ml/20 g wet tissue. The complete gastrointestinal tract from each animal had an average mass of 2.8 g ($n = 6$ mice). The phosphatase inhibitor was used at a concentration of 1 ml/100 ml of homogenization buffer.] The protease inhibitor (P8340, Sigma) contained AEBSF, aprotinin, bestatin, E-64, leupeptin hemisulfate, and pepstatin. The phosphatase inhibitor contained cantharidin and microcystin LR (P2850, Sigma) that specifically inhibited serine phosphatases like PP2A and PP1.

Subcellular fractionation. The method used for varicosity isolation is summarized in Fig. 1 and was similar to protocols described earlier for varicosities preparation in intestine (10, 27). Samples were centrifuged at 1,000 *g* for 10 min at 4°C to remove undissociated tissue (pellet P1) that was washed once in buffer, the pellet was discarded, and the combined supernatants were further centrifuged at 4,000 *g*. The pellet P2 obtained after spinning at 4,000 *g* represented the nuclear fraction and the supernatant was the cytoplasmic fraction. This supernatant was subjected to ultracentrifugation at 25,000 rpm at 4°C for 30 min. The pellet P3 obtained was the varicosity fraction, whereas the supernatant represented the microsomal fraction. Pellet P3 was resuspended in 400 μl of Krebs buffer (111 mM NaCl, 26.2 mM $NaHCO_3$, 1.2 mM NaH_2PO_4, 4.7 mM KCl, 1.8 mM $CaCl_2$, 1.2 mM $MgCl_2$, 11 mM glucose, gassed with 95% O_2 and 5% CO_2 to maintain a pH of 7.4) and subjected to further purification. The homogenization buffer contained EGTA to facilitate low levels of calcium during the initial phases of low-velocity centrifugation. The low calcium was deemed necessary for appropriately sealing the varicosity membranes. Furthermore, before the P3 pellet was subjected to ultracentrifugation, it was resuspended in Krebs buffer that was replete with divalent calcium. In all experiments pertaining to studying nNOS phosphorylation, varicosity preparations were made by omitting EGTA in the homogenization buffer. The P3 extract was layered on a 0.8/1.2 M sucrose gradient and subjected to sucrose gradient ultracentrifugation at 58,000 rpm for 1 h at 4°C. Intact varicosities that formed a cloudy or ringlike structure at the interface of the two differing sucrose concentrations were carefully collected with a 200-μl pipette tip, diluted in Krebs buffer and centrifuged at 12,000 rpm for 5 min at 4°C to pellet down varicosities. Varicosities were stored at −80°C until further experiments.

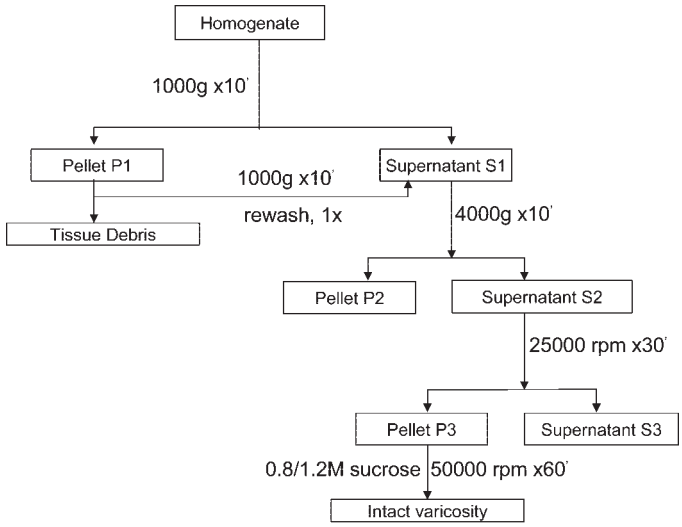

Fig. 1. Protocol for isolation of nerve varicosities from mouse gut. Different velocities of cold ultracentrifugation and sucrose gradient purification were used to obtain varicosities.

Transmission electron microscopy. Varicosity samples were fixed immediately after isolation in a fixative composed of 2% paraformaldehyde and 2.5% glutaraldehyde in 0.1 M sodium cacodylate buffer (pH 7.4) at room temperature and, after an hour, centrifuged at 12,000 rpm for 5 min. The resultant pellet was processed at the Electron Microscopy Core Facility at Harvard Medical School in the following sequence: washed thrice in buffer containing 1% osmium tetroxide-1.5% aqueous potassium ferrocyanide for 1 h at room temperature, in water three to four times, with 1% uranyl acetate-maleate buffer for 30 min, and again with water thrice. It was then dehydrated with ethyl alcohol (70%) for 15 min, 90% for another 15 min, and finally with 100% alcohol for 15 min and repeated one more time. Next, it was treated with propylene oxide for an hour, embedded in a ratio of 1:1 TAAB epon resin at room temperature for 2–3 h, and then transferred to a mold filled with freshly mixed TAAB epon. It was then poly-

Table 1. *Antibodies used*

Antibody	Target	Dilution	Usage	Host	Source	Rationale
Anti-COOH-terminal nNOS1422–1433	nNOS (AA 1422–1433)	1:100	WB, IP	Rabbit	Alexis	Total nNOS
Anti-NH_2-terminal nNOS1–20	nNOS (AA 1–20)	1:100	WB	Rabbit	Santa Cruz	nNOS containing PDZ domain in N-terminal end
Anti-serine847-PnNOS	Serine 847-phosphorylated nNOS	1:50	WB, IP	Rabbit	Santa Cruz	nNOS phosphorylated at serine 847
Anti-CaM	Calmodulin	1:100	IP, WB	Mouse	Upstate	Calmodulin-bound nNOS
Anti-synaptophysin	Synaptophysin	1:100	WB, IHC	Mouse	Febgennix	Synaptosome

The appropriate secondaries were used at a tenfold dilution compared to the primary, except for phospho-serine 847-nNOS where a fivefold dilution (1 in 250) was used compared to the primary. nNOS, neuronal nitric oxide synthase; CaM, calmodulin; WB, Western blot; IP, immunoprecipitation; IHC, immunohistochemistry.

merized at 60°C for 48 h in an oven. Ultrathin sections (60–80 nm) were cut using a Reichert Ultracuts microtome and observed under a JEOL 1200 EX transmission electron microscope.

Fluorescence microscopy. After isolation, varicosity samples were fixed immediately in a fixative (Histochoice, Amresco) and incubated overnight at 4°C. This solution was then spun down and the resultant pellet was used for immunostaining. The varicosity pellet was washed with Tween-PBS thrice for 15 min, and then further washed with 70% alcohol for at least 10 min, followed with a quick wash with PBS-Tween. The pellet was resuspended in a primary antibody solution ($nNOS_{1422–1433}$ and synaptophysin, respectively) and incubated overnight at 4°C in a shaking incubator. Next, the samples were spun and the varicosity pellet was resuspended in washing solution PBS-Tween for 5 min, after which it was spun down and an appropriate secondary antibody solution (donkey anti-rabbit Texas Red and goat anti-rat Cy5, respectively) was added. The pellet was incubated with secondary antibody under shaking conditions for 2 h, spun down, and washed with PBS-Tween for 5 min. The samples were mounted on clean glass slips and observed with a fluorescent microscope (Olympus).

Preparation of the varicosity extracts for Western blots. Isolated varicosities were centrifuged at 12,000 rpm for 5 min at 4°C after addition of Cellytic buffer (Sigma) to obtain proteins in solution. The extracts were processed at low temperature (4°C) or heat treated at 37°C for 10 min. For the low-temperature processing, 60–80 μg of protein in Laemmli buffer [0.125 M Tris·HCl (pH 6.8), 4% (wt/vol) SDS, 10% (vol/vol) 2-mercaptoethanol, 20% (wt/vol) glycerol, and 0.02% bromophenol blue] at 4°C was used for SDS-PAGE. The low-temperature process was used to identify nNOS dimers and monomers in the native state because low temperature is known to prevent monomerization of nNOS dimers (18). Heat-treated samples were processed as follows: protein was treated with Laemmli buffer for 10 min at 37°C and immediately subjected to electrophoresis; 35 μl of protein samples were loaded into each lane during electrophoresis.

SDS-PAGE of varicosity extracts. Electrophoresis was carried out by using Bio-Rad mini-protean II system or a Wako gel casting system. Preliminary experiments were carried out in 4–20% gradient polyacrylamide gels, and confirmatory gels were run by separating proteins in 7.5% gels that provided efficient resolution of the higher molecular weight proteins examined in the present study. Pilot experiments were performed for standardization of the type of gel, the run time, the concentrations of the primary and secondary antibodies, and the incubation times.

Total protein concentrations were measured using Bradford method at 595λ optical density. For almost every experiment, 60 μg of protein was loaded for low-temperature SDS-PAGE. The samples were subjected to SDS-PAGE for a variable period of time (between 2 and 5 h, depending on the migration of the molecular weight marker) at 90 V in cold-room at 4°C. For all electrophoresis, Precision Plus (Bio-Rad) molecular weight marker was used to identify migration patterns. All experiments were performed with appropriate positive controls and loading controls were evaluated for homogeneity of results. Additionally, for each experiment, at least three different sets of varicosity extracts were used (each extract from a set of 3–10 mice) and electrophoresis was always repeated more than thrice to confirm the findings.

After electrophoresis, the separated proteins were transferred to polyvinylidene difluoride membranes (Bio-Rad) overnight at 30 V at 4°C, and the efficiency of immunoblotting was checked by Ponceau staining. Blots (membranes with separated proteins) were washed with Tris-buffered saline (Bio-Rad) with Tween (TBST) for 10 min and blocked for 1 h in 5% nonfat milk-TBST (unless otherwise mentioned) at room temperature. The primary antibody was added in the blocking solution at differing dilutions (see Table 1) and the blot was probed with this primary antibody on a rocking platform overnight at 4°C. For experiments probing phospho-nNOS, the blocking solution used was 5% BSA, and the same solution was used for diluting the antibodies. Milk was avoided as the blocking solution to reduce background because milk proteins are abundantly phosphorylated. The blot was subsequently washed with washing buffer for 1 h and an appropriate secondary antibody conjugated to chemiluminescent horseradish peroxidase was added at a 5- to 10-fold dilution to the primary antibody (see Table 1) and incubated for 1 h on a rocking platform at room temperature. After the blot was washed with TBST thrice for 20 min each per wash, immunolabeled blots were developed with a premixed chemiluminescent developer enhanced chemiluminescent reagent (Upstate). Blots were exposed to a chemiluminescent detection film in the dark for variable time periods and processed in an X-ray developer machine (Kodak X-OMAT 2000A).

Immunoprecipitation studies. Solubilized varicosity extracts in Cellytic buffer (Sigma) were centrifuged and the supernatant was diluted to a starting protein concentration of 1 mg/ml. The buffer used resembled composition of the standard RIPA buffer and contained protease inhibitors and 50 mM Tris·HCl pH 7.5 (5 ml), 150 mM NaCl (3.75 ml), 1% Nonidet P40, and 0.5% sodium deoxycholate (2.5 ml). A homogenous suspension (50 μl) of protein G-agarose (A/G) was added to 1 ml varicosity extract (1 mg protein/ml) and incubated overnight at 40% speed at 2–8°C on a rotating rocker (Glas-Col, Terre Haute, IN). Varicosity extracts with beads were centrifuged at 12,000 *g* for 20 s in a microfuge. After the supernatant was transferred to fresh tubes, 10 μg of the specific antibody was added and gently rocked overnight at 2–8°C. Antibodies used for immunoprecipitation were anti-$nNOS_{1422–1433}$, which detected all forms of nNOS, and anti-CaM antibody, which detected association of CaM with nNOS. After the complexes were collected by centrifugation at 12,000 *g* for 20 s in a microfuge, the supernatant was carefully aspirated and used for further experiments. The beads were washed thrice with 1 ml of lysis buffer and spun at 12,000 *g* for 2 min each time, and 2X loading buffer (the Laemmli buffer) was added to these protein A/G beads on ice to isolate protein from the beads. Immunoprecipitated protein was subjected to low-temperature SDS-PAGE and probed with different antibodies. To identify nNOS isoforms in CaM-lacking nNOS, the supernatant after CaM immunoprecipitate was removed and concentrated by use of a centrifugal filter device at 4,000 *g* for 30 min in a swinging-bucket-type ultracentrifuge (Sorvall RT) at 4°C. The filter devices had low-binding Ultracel membranes with a nominal molecular mass limit of 50 kDa (less than twice the size of the least anticipated molecular weight in the present set of experiments) (Amicon Ultra-4, Millipore). The retentate (containing proteins with molecular mass >50 kDa) was subjected to further electrophoresis and hybridized with serine 847-phospho-nNOS antibody.

Quantification of blots. After developing, the blots were scanned with unaltered luminosity so that the optical density remained unaffected. The peak intensity of a user-identified band was evaluated by using the NIH program ImageJ. The band intensity was expressed as arbitrary units, and mean expression was obtained by averaging intensity values of three to nine different lanes for each experiment, each lane representing gut varicosity extract from three to ten mice.

Functional studies of in vitro NO production. NO production by various fractions of nNOS (using varicosity extracts and immunoprecipitated samples with specific antibodies) was measured by using DAF-2 (diaminofluorescein). This dye is highly sensitive to NO and binds to it to form a fluorescent product. This product can be detected at 495/515 nm in a spectrofluorometer (Bio-Rad). Varicosity pellets were dissolved in a buffer composed of 50 mM Tris·HCl, pH 7.4, and protease inhibitors. One hundred microliters of this sample were mixed with 100 μl of assay buffer. The assay buffer consists of 55 mM HEPES, 20 mM Tris·HCl, pH 7.4, 2 mM L-arginine, 0.8 mM dithiothreitol, 0.8 μM NADPH, 1 mM $MgCl_2$, 1 mM $CaCl_2$, 0.5 μM CaM, 0.8 μM riboflavin monophosphate, 6 μM (6R)-5,6,7,8-tetrahydrobiopterin (BH_4), 0.8 μM flavin-adenine dinucleotide, and protease inhibitors. DAF-2 (10 μM) was also added to this reaction mixture. The assay was performed in different experimental conditions using nNOS inhibitors N^G-nitro-L-arginine methyl ester (L-NAME) and

7-nitroindazole (7-NI) and by omitting L-arginine in the buffer. Additionally, heat-treated samples were also assayed for NO production. The NO donor Nor-3 was used for plotting known NO levels as a standard graph, and this was used to calculate values of unknown biological samples (13).

Statistical analysis. Expression values of enzymes or enzymatic activities were represented as means ± SE. Comparison of means was performed by using *t* statistics with MS Excel.

RESULTS

Identification of nitrergic varicosities. The identity of varicosities in the enriched fraction was confirmed by transmission electron microscopy. Figure 2*A* shows transmission electron microscopic appearance of varicosities containing secretory granules and diffuse cellular contents. Average size of varicosities ranged between 0.5 and 2 μm. The majority (~90%) of varicosities showed secretory vesicles with a granular appearance. Figure 2*B* shows phase contrast image of the varicosity preparation mounted on a glass slide. Varicosities immunostained with anti-nNOS$_{1422–1433}$ confirmed their nitrergic identity (Fig. 2*C*). nNOS and synaptophysin were colocalized indicating that the isolated structures containing nNOS were neural varicosities (Fig. 2*D*). The nNOS/synaptophysin colocalization was also confirmed by electrophoresis of the varicosity extracts and by immunoblotting with anti-nNOS$_{1–20}$ and anti-synaptophysin antibodies (Fig. 2*E*).

Anti-nNOS$_{1422–1433}$ antibody reactive nNOS. Immunoblots probed with anti-nNOS$_{1422–1433}$ antibody that is specific for the COOH-terminal end of nNOS identified all isoforms of nNOS because the COOH-terminal regions of all isoforms of nNOS are identical. The COOH-terminal antibody identified three nNOS bands of ~320, 250, and 155 kDa on low-temperature SDS-PAGE (Fig. 3). The relative proportions of nNOS 320-, 250-, 155-, and 135-kDa bands in cold-processed SDS-PAGE were determined densitometrically as 1:0.57 ± 0.44:1 ± 0.99:0. The relative proportion of 320- and 250-kDa bands of 1:0.57 indicated that 320-kDa nNOS made up the bulk of nNOS dimer in the varicosities and the 250-kDa fraction was only about half of the 320-kDa fraction.

The warm (37°C) SDS in the Laemmli buffer showed no 320- and 250-kDa bands, which were replaced by 155- and 135-kDa nNOS bands (Fig. 3). These observations are consistent with the fact that the 320- and 250-kDa bands in low-temperature SDS-PAGE were dimers that appear as 155- and 135-kDa monomers, respectively, on heat treatment.

Anti-nNOS$_{1–20}$ antibody reactive nNOS. To identify the nNOS bands containing PDZ domain, the Western blots were probed with anti-nNOS$_{1–20}$ antibody (specific for the NH_2-terminal end of nNOS) that reacts with the PDZ binding site of nNOS. The NH_2-terminal antibody identified 320 and 155-kDa bands on low-temperature SDS-PAGE and only 155-kDa nNOS band on heat-treated SDS-PAGE (Fig. 3). The NH_2-terminal nNOS antibody did not recognize the 250- and 135-kDa bands that represented nNOS lacking the PDZ binding domain. The relative proportion of nNOS$_{1–20}$ reactive nNOS was 1:1.8 ± 1 for the 320-kDa dimer and 155-kDa monomer, respectively, on cold-temperature SDS-PAGE. These observations suggest that over half of nNOSα in the varicosities in the resting state exist as monomers.

CaM association with nNOS isoforms. CaM association of nNOS is critical for its catalytical activity. To identify nNOS fractions that were associated with CaM in enteric nerve varicosities, immunoprecipitation was performed with anti-nNOS$_{1422–1433}$ antibody and the immunoblots were probed with an anti-CaM antibody. Anti-CaM antibody detected a 320-kDa band in the immunoprecipitate (Fig. 4). Heat treatment showed a band at 17 kDa representing the CaM dissociated from its bound state with nNOS (Fig. 4). The 250- and

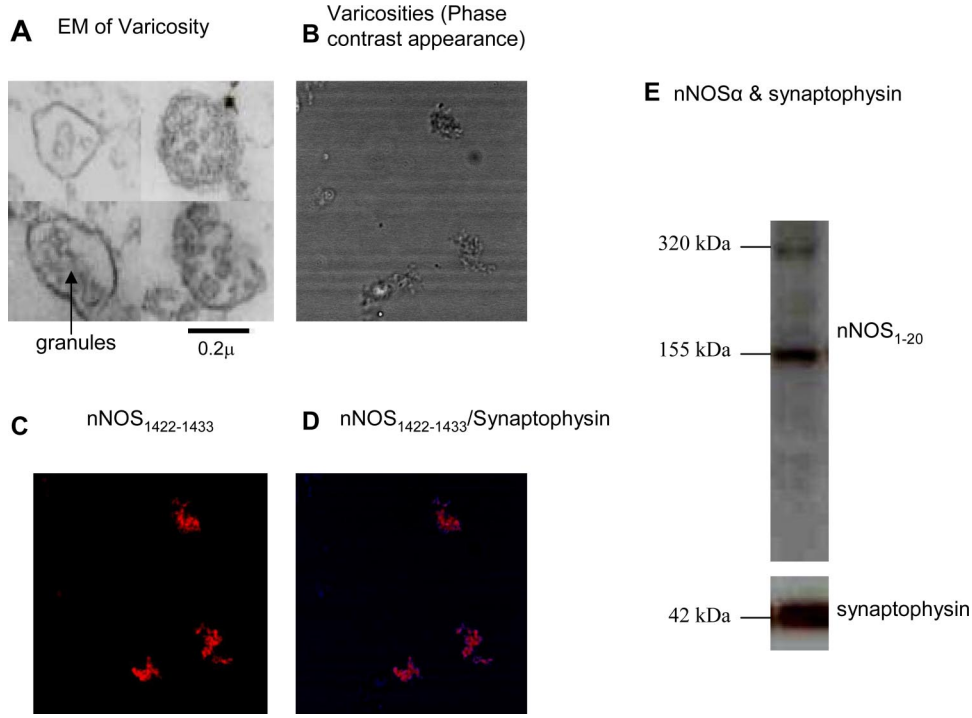

Fig. 2. Identification of varicosities isolated from the gut. *A*: transmission electron microscopy demonstrated ~2 μm varicosity with dense granules and diffuse cellular contents. *B*: phase contrast appearance of smears of varicosities laid out on clean glass slips. Many enteric varicosities were immunopositive for neuronal nitric oxide synthase (nNOS; pseudocolored red) whereas others were nNOS negative (*C*) and colocalized with synaptophysin (pseudocolored blue at the rim of the varicosities) (*D*), a synaptic marker, when varicosity smears were examined under fluorescence microscopy. nNOS/synaptophysin colocalization was also demonstrated by immunoblotting (*E*).

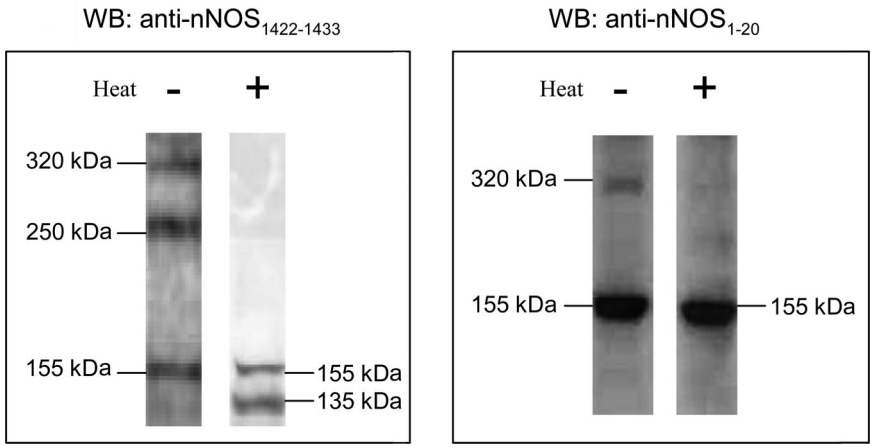

Fig. 3. Identification of different nNOS forms in varicosity extracts. *Left*: varicosity extracts under nondenaturing conditions (on ice) immunoblotted with anti-$nNOS_{1422–1433}$ antibody showed dimers and monomer at 320, 250, and 155 kDa. Heat-treated (37°C) extract probed with the same antibody detected monomers at 155 and 135 kDa. *Right*: the nNOSα splice variant was identified in the varicosity extract by anti-$nNOS_{1–20}$ antibody in the cold condition that detected a 320-kDa dimer and a 155-kDa monomer band. Heat-treated extract probed with anti-$nNOS_{1–20}$ antibody detected only the monomer at 155 kDa. Note that both splice variants of nNOS, nNOSα and nNOSβ, are present in the gut nerve terminals.

155-kDa bands in the varicosity extracts were not found to be associated with CaM.

To further confirm the above findings, we performed a reverse experiment using varicosity immunoprecipitation with CaM and probing the immunoprecipitate with anti-$nNOS_{1422–1433}$ antibody. This process revealed only the 320-kDa band on Western blotting. Neither the 250-kDa nor 155-kDa bands were identified in the CaM IP at low-temperature SDS-PAGE (Fig. 4). CaM immunoprecipitate on heat-treated SDS-PAGE showed a 155-kDa band that presumably represented the monomer of the 320-kDa nNOS (Fig. 4).

Identification of serine 847-phosphorylated nNOS. One of the important mechanisms of regulation of CaM binding to nNOS is phosphorylation of the nNOS enzyme at serine 847 that inhibits CaM binding. Therefore we examined the presence of serine 847-phosphorylated nNOS isoforms in the native varicosities in the gut in the presence of inhibitors of serine phosphatases (PP2A). Immunoblots of varicosity extracts probed with serine 847-phosphorylated nNOS antibody revealed 320-, 250-, and 155-kDa bands at low-temperature SDS-PAGE. Heat treatment of varicosity protein extracts with Laemmli buffer at 37°C demonstrated only the 155-kDa band (Fig. 5).

Serine 847 phosphorylation state of CaM-bound and CaM-lacking nNOS. To determine serine 847 phosphorylation state of nNOS isoforms of CaM-bound and CaM-lacking fractions in the varicosities, varicosity extracts were immunoprecipitated with anti-CaM antibody and the supernatant was concentrated by using a membrane dialyzer at high speed; this retentate (containing proteins >50 kDa) was subsequently hybridized with serine 847-phospho-nNOS antibody. CaM-immunoprecipitated nNOS showed no serine 847-phosphorylated nNOS (Fig. 5). On the other hand, the supernatant that was obtained after the initial immunoprecipitation with the CaM antibody, representing the CaM-lacking nNOS fraction, revealed bands at 320, 250, and 155 kDa when probed with the serine 847-phospho-nNOS antibody (Fig. 5). These results suggest that the CaM-lacking nNOS contain nNOS isoforms that were phosphorylated at serine 847. The serine 847 phospho-nNOS fraction in the supernatant after CaM immunoprecipitate showed relative proportions of 320, 250, and 155 kDa of 1:1.08 ± 1.26:1.79 ± 1.2 ($n = 3$, each set of varicosity samples was prepared from 6 mice).

NO production by different nNOS isoforms. As shown in Fig. 6, immunoprecipitates of varicosity extracts with CaM showed that the fraction of CaM-bound nNOS actively produced NO in an in vitro assay (49.19 ± 1.47 pmol·30 min^{-1}·mg $protein^{-1}$). This NO production was significantly suppressed after pharmacological treatment with L-NAME ($P < 0.05$), a drug that inhibits all forms of nNOS enzyme. The NO production was also significantly suppressed by 7-NI ($P < 0.05$), a drug that inhibits nNOS enzyme by inhibiting BH_4 and

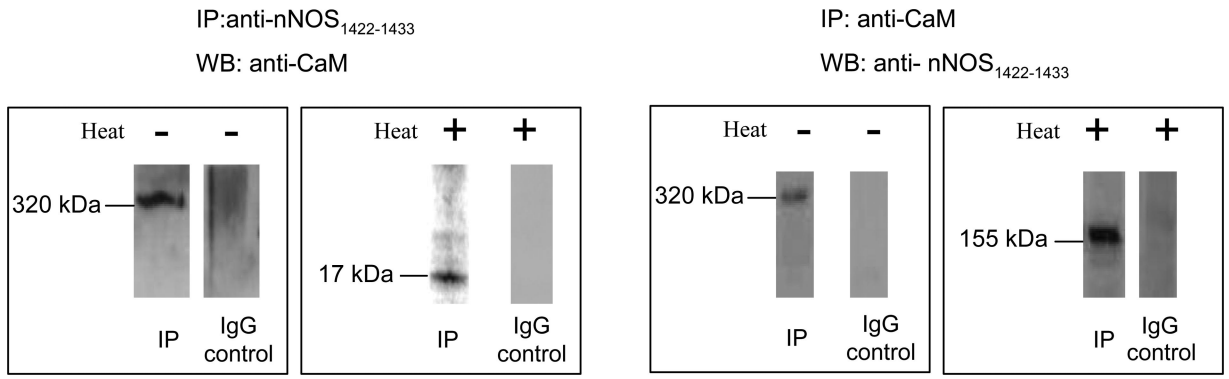

Fig. 4. CaM-associated and CaM-lacking fractions of nNOS. *Left*: $nNOS_{1422–1433}$ immunoprecipitate (IP) probed with anti-calmodulin (CaM) antibody. The 320-kDa band shows that CaM is bound to the nNOS immunoprecipate. Heating the immunoprecipitate sample dissociated the CaM that was bound to nNOS, which was detected as a 17-kDa band. *Right*: CaM immunoprecipitate probed with anti-$nNOS_{1422–1433}$ antibody. In the native state of the nerve terminals in gut, CaM binds only to nNOS dimer at 320-kDa. Note that CaM does not associate with the nNOSβ dimer or the nNOSα monomer.

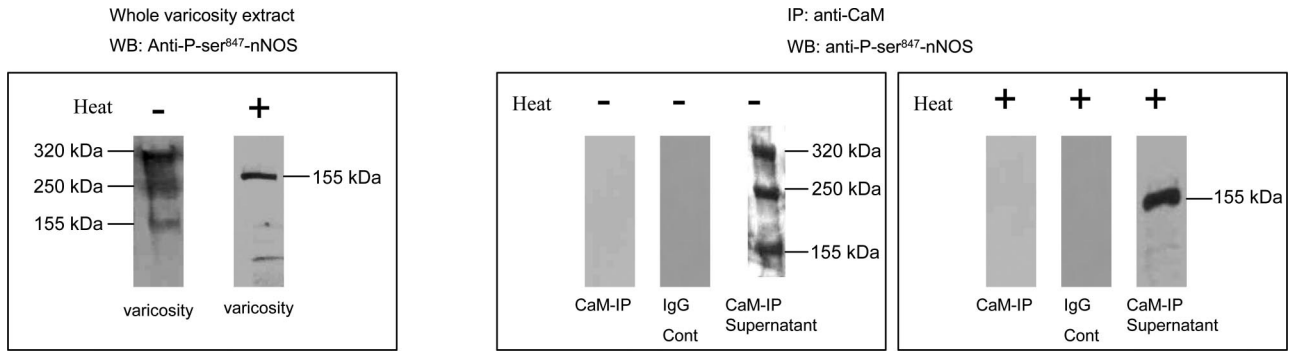

Fig. 5. Phosphorylation patterns of nNOS in gut nerve terminals. *Left*: phosphorylation states of nNOS in varicosity extracts. In native condition, portions of nNOS α and β dimers and nNOSα monomers were phosphorylated. Immunoblots of nondenatured varicosities extracts revealed bands at 320, 250, and 155 kDa when probed with serine 847-phospho-nNOS, and mild heat treatment showed prominent band at 155 kDa. *Right*: phosphorylation states of CaM-bound and CaM lacking nNOS. CaM immunoprecipitate was probed with anti-phospho-serine 847-nNOS antibody. No signal was detected. These experiments showed that CaM-bound nNOS was not phosphorylated at serine 847. The floating fraction obtained after CaM immunoprecipitation was probed with anti-phospho-serine 847-nNOS antibody. The floating fraction obtained after precipitating varicosity extracts with anti-CaM antibody represented the pool of nNOS that did not bind to CaM. This fraction was concentrated by use of a membrane dialyzer at high centrifugation speeds and the retentate was probed with phospho-serine 847-nNOS antibody. Under nondenaturing conditions (4°C, SDS-PAGE), 320-, 250-, and 155-kDa bands were visualized, representing serine 847-phospho-nNOS α dimer, β dimer, and α monomer, respectively. Mild heat treatment (37°C, 10 min) showed a 155-kDa band. Immunoprecipitation with mouse IgG served as negative controls.

consequently disrupting nNOS dimer formation. NO was not produced when L-arginine was removed from the assay mixture. These studies showed that CaM-associated nNOS was catalytically active. In contrast, precipitates of varicosity extracts with serine 847-phosphorylated-nNOS antibodies (i.e., serine-phosphorylated nNOS) showed very low levels of NO production (9.60 ± 1.45 pmol·30 min^{-1}·mg $protein^{-1}$). The nNOS inhibitors L-NAME and 7-NI did not further inhibit NO production in these samples ($P > 0.05$). Additionally, the floating fraction obtained after CaM immunoprecipitate of the varicosity extract showed scant or no production of NO in the in vitro assay, showing that the CaM-lacking nNOS in the supernatant could not generate NO. These data indicate that serine 847-phosphorylated nNOS was catalytically inactive. Heat-treated varicosity samples (37°C) did not show any detectable level of NO during the functional assay, suggesting that monomers of nNOS were ineffective in NO synthesis.

DISCUSSION

This study shows that in the enteric varicosity extracts *1*) nNOS was present as 320-, 250-, 155-, and 135-kDa bands; *2*) these bands represented dimers and monomers of α and β isoforms of nNOS, respectively; *3*) 320-kDa nNOSα dimer existed in both CaM-bound and CaM-free forms; *4*) CaM-associated nNOSα dimer was catalytically active, whereas the CaM-lacking nNOSα dimer was catalytically inactive and was phosphorylated at serine 847; *5*) 155-kDa nNOSα monomer and 250-kDa nNOSβ dimers lacked CaM and were also catalytically inactive.

Various isoforms of nNOS, namely α, β, γ, μ, and nNOS2 isoforms, are produced by the posttranscriptional splicing of nNOS mRNA (22, 23). The dimers of nNOS α, β, γ, μ, and nNOS2 are known to have approximate molecular masses of 320, 250, 250, 330, and 288 kDa, respectively, and their monomers have molecular masses of ~155, 135, 125, 165, and 144 kDa, respectively (2). Because of this proximity, approximate determinations of molecular masses of the bands do not adequately distinguish various isoforms of nNOS. NH_2-terminal nNOS antibody was used to distinguish nNOS isoforms that contain complementary PDZ binding domain from those lacking it. Hence, the 320-kDa band could be nNOSα, nNOSμ, or nNOS-2 that possess PDZ binding domain. On the other hand, the 250-kDa band could be either nNOSβ or nNOSγ that lack the PDZ binding domain (1).

However, studies of tissue localization, mRNA expression, and functional assay helped to identify the nature of these nNOS isoforms. Tissue localization studies have shown that nNOSα is localized to neurons and nNOSμ is localized to striated and cardiac muscles (2, 14). A detailed study of nNOS mRNA splice variants and proteins in gut nerve-muscle preparation have shown that both nNOS mRNA and protein for nNOSα are localized in the gut, whereas there was no expression of nNOSμ (22). These studies supported the view that the 320-kDa band visualized in the present study was not nNOSμ. On the other hand, nNOS-2 has no enzymatic activity (2). However, the 320-kDa band in our studies was catalytically active in an in vitro assay, suggesting that it was not nNOS-2. Therefore, by exclusion, it appears that the 320-kDa band represented nNOSα. The 250-kDa band did not react with the NH_2-terminal nNOS antibody and therefore represented PDZ domain-lacking nNOSβ or nNOSγ isoforms. Saur et al. (22, 23) have shown that whereas mRNA for nNOSβ is present in certain regions of the gut, mRNA for nNOSγ is never expressed. Therefore, it appears that the 250-kDa fraction represented nNOSβ.

Since nNOSα contains a PDZ-binding domain, nNOSα is the likely candidate enzyme involved in nitrergic neurotransmission because of its ability to localize at the cell membrane (2). Localization to the varicosity membrane places it in close proximity to calcium channels and hence may allow prompt response to calcium influx on activation of the nerve terminal. The critical role of nNOSα in nitrergic neurotransmission is also supported by functional studies. For example, it has been shown that loss of nNOSα in genetically engineered mice lacking exon 2 of the nNOS gene (8) shows loss of nitrergic slow inhibitory junction potentials in the gut (15) and phenotypic abnormalities like pyloric stenosis consistent with the loss of nitrergic neurotransmission (16, 26). Moreover, the

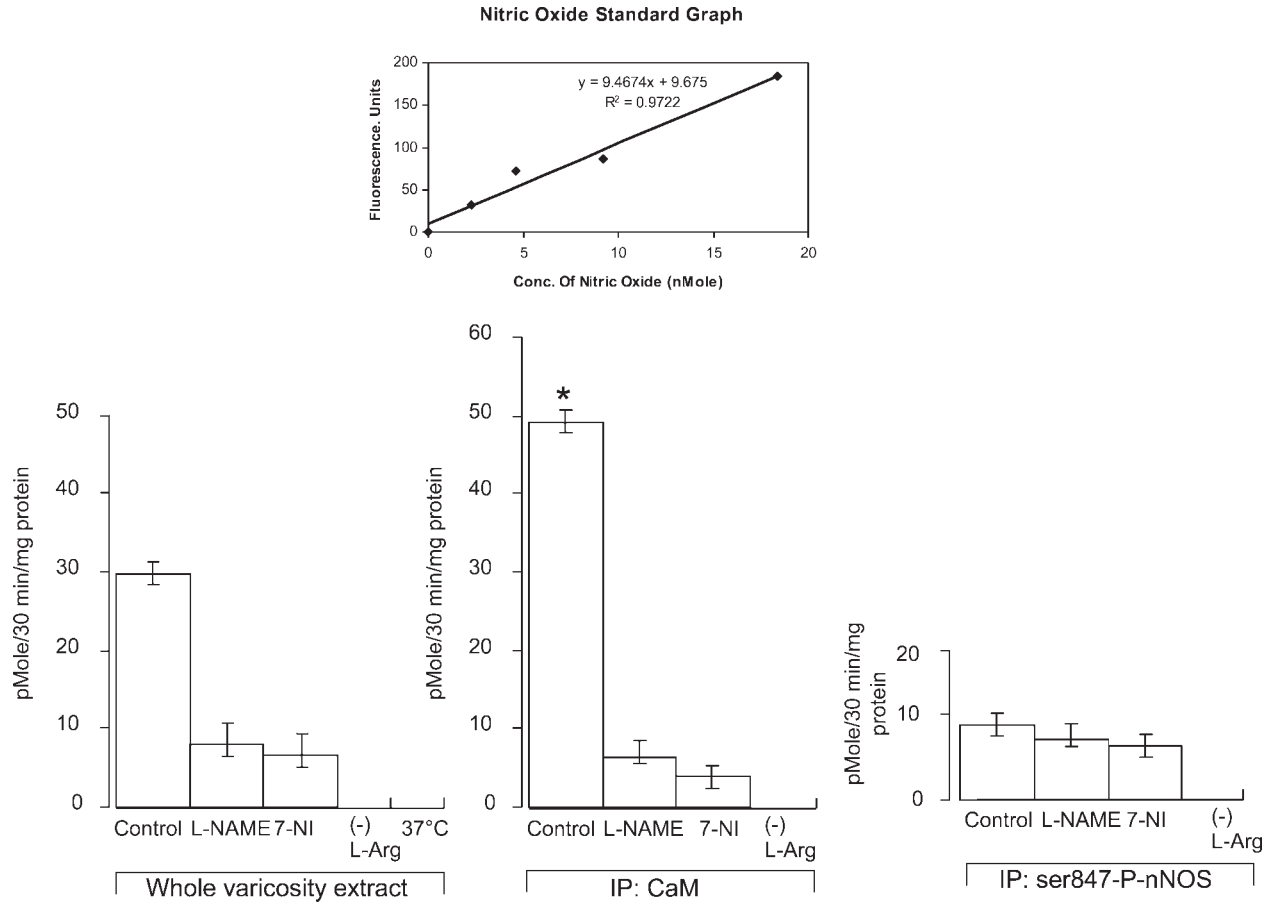

Fig. 6. Quantification of nitric oxide production by different nNOS fractions in mouse nerve terminals in vitro. Histograms represent activity profiles of in vitro nitric oxide synthesis as assessed by a fluorimetric assay using diaminofluorescein in whole varicosity extracts, CaM immunoprecipitate, and phospho-serine 847-nNOS immunoprecipitate samples. For each of the categories, the nitric oxide assays were performed in quadruplicates. A nitric oxide donor, nor-3, was used to calculate the standard graph from which nitric oxide production in unknown biological samples was computed (shown at *top*). Note the robust production of nitric oxide by the CaM immunoprecipitates compared with serine 847-P-nNOS immunoprecipitates. Also note that heat (37°C) and omission of L-arginine from the samples resulted in total absence of in vitro NO synthesis.

phenotypic changes due to loss of nNOSα in exon2 nNOS knockout mice are similar to loss of total nNOS activity due to deletion of exon 6 of nNOS (7, 8).

Calcium-CaM (Ca-CaM) binding to nNOS is critical for its enzymatic activity (19). The nNOS molecule contains an autoinhibitory hinge loop that links its COOH-terminal reductase domain to the NH_2-terminal oxygenase domain and inhibits its enzyme catalysis (2). Ca-CaM binds to a site (724–757 amino acids of nNOSα) that is adjacent to this inhibitory loop (amino acids spanning 831–872). The binding of Ca-CaM to this site displaces the inhibitory loop and forms a bridge between oxygenase and reductase domains and promotes the flow of electrons from the reductase domain to oxygenase domain, which is imperative in increasing the rate of enzyme catalysis. NO formation is critically dependent on this intersubunit electron transfer (17, 18) and, consequently, calcium-activated CaM-nNOS tetramer is necessary for catalytic activity of nNOS.

This study showed that the gut varicosities contained both CaM-bound and CaM-lacking nNOSα fractions. It further documented that CaM-associated nNOS was catalytically active and produced NO in an in vitro assay system, whereas CaM-lacking nNOSα was inactive. The regulation of CaM-associated and CaM-lacking fractions of nNOS may be of critical importance in the regulation of the amount of NO synthesis and release during nitrergic neurotransmission in the gut. One of the important mechanisms determining whether CaM binds to nNOS and activates it is its state of phosphorylation of serine at position 847 (3, 19). An important finding of the present study was that a fraction of nNOS in the gut nerve terminals is serine 847 phosphorylated. This observation is similar to our previous preliminary report of serine 847 phosphorylated nNOS using a different anti-serine 847-phospho-nNOS antibody (NP847) (20). Since serine 847 is present within the autoinhibitory loop of the nNOS enzyme, phosphorylation of serine 847 of nNOSα prevents Ca-CaM binding and prevents displacement of the inhibitory loop even in the presence of high concentrations of Ca-CaM and keeps the enzyme inactive (19). Phosphorylation is a rapid cellular event and serine 847 dephosphorylation/phosphorylation of nNOSα in the enteric nerve terminals may facilitate a rapid turnover between active and inactive enzyme forms.

The present study documented by using an in vitro assay that whereas CaM-bound nNOSα actively synthesized NO, serine 847-phosphorylated nNOS was not CaM bound and lacked the ability to synthesize NO. Thus, in the gut varicosities, serine

847 phosphorylation of nNOSα may be an important mechanism for regulation of pools of inactive and active nNOS isoforms. In addition to CaM-lacking nNOSα dimer, the varicosities were also found to contain CaM-lacking nNOSα monomers and nNOSβ isoforms, all of which were serine 847 phosphorylated and were catalytically inactive. Thus, although nNOSβ and nNOSα monomers do not contribute to the enzymatic activity, they add to the total nNOS present in the gut nerve terminals. Function of the nNOSβ isoform in nitrergic neurotransmission, if any, is not known. However, it has been suggested that this splice variant of nNOS may participate in residual penile erection in mice lacking nNOSα (9).

The equilibrium between the catalytically active nNOSα dimer and catalytically inactive nNOSα monomer has been reported to correlate with functional nitrergic responses in the stomach (6). In endogenous system, this equilibrium is regulated by BH_4, heme, and L-arginine (12). The dimer-monomer equilibrium of nNOSα may also regulate nitrergic neurotransmission.

In summary, the present study showed that, in mouse gastrointestinal nerve terminals, nNOSα existed as unphosphorylated, CaM-associated and serine 847-phosphorylated, but CaM-deficient dimers. The CaM-associated nNOSα dimer was catalytically active and yielded NO in vitro. On the other hand, the serine 847-phosphorylated nNOSα dimer and monomers of nNOSα were catalytically inactive. During calcium influx in the nerve varicosities in the gut, only the catalytically active nNOSα (the enzyme dimer that is bound to CaM and not phosphorylated at its serine 847) can serve as an immediate source for catalysis of NO production. The measurement of total nNOS in nerve terminals may not provide adequate information on the state of nitrergic neurotransmission. The present study is the first attempt to address the regulation of nitrergic neurotransmission in the gut nerve terminals, the precise sites of NO synthesis during anterograde inhibitory neurotransmission in the gastrointestinal tract. Regulation of the equilibrium between catalytically active and inactive nNOSα pools in the enteric varicosities may be critically important in regulating nitrergic neurotransmission. Further studies of time-dependent changes in the chemical nature of different nNOS isoforms after nerve stimulation are needed to test this hypothesis.

ACKNOWLEDGMENTS

We thank Louise Trakimas of the Electron Microscopy Core Facility at the Harvard Medical School Division of Cell Biology, Dr. Hemant Thatte for help with imaging studies, and Dr. MaryRose Sullivan for helpful suggestions.

GRANTS

This work was supported by a National Institute of Diabetes and Digestive and Kidney Diseases Grant (DK-062867) and a Merit Review Award from the Office of Research and Development, Medical Research Services, Department of Veterans Affairs.

REFERENCES

1. **Abdelmoity A, Padre RC, Burzynski KE, Stull JT, Lau KS.** Neuronal nitric oxide synthase localizes through multiple structural motifs to the sarcolemma in mouse myotubes. *FEBS Lett* 482: 65–70, 2000.
2. **Alderton WK, Cooper CE, Knowles RG.** Nitric oxide synthases: structure, function and inhibition. *Biochem J* 357: 593–615, 2001.
3. **Bredt DS, Ferris CD, Snyder SH.** Nitric oxide synthase regulatory sites. Phosphorylation by cyclic AMP-dependent protein kinase, protein kinase C, and calcium/calmodulin protein kinase; identification of flavin and calmodulin binding sites. *J Biol Chem* 267: 10976–10981, 1992.
4. **Bult H, Boeckxstaens GE, Pelckmans PA, Jordaens FH, Van Maercke YM, Herman AG.** Nitric oxide as an inhibitory non-adrenergic non-cholinergic neurotransmitter. *Nature* 345: 346–347, 1990.
5. **Esplugues JV.** NO as a signalling molecule in the nervous system. *Br J Pharmacol* 135: 1079–1095, 2002.
6. **Gangula PR, Maner WL, Micci MA, Garfield RE, Pasricha PJ.** Diabetes induces sex-dependent changes in neuronal nitric oxide synthase dimerization and function in the rat gastric antrum. *Am J Physiol Gastrointest Liver Physiol* 292: G725–G733, 2007.
7. **Gyurko R, Leupen S, Huang PL.** Deletion of exon 6 of the neuronal nitric oxide synthase gene in mice results in hypogonadism and infertility. *Endocrinology* 143: 2767–2774, 2002.
8. **Huang PL, Dawson TM, Bredt DS, Snyder SH, Fishman MC.** Targeted disruption of the neuronal nitric oxide synthase gene. *Cell* 75: 1273–1286, 1993.
9. **Hurt KJ, Sezen SF, Champion HC, Crone JK, Palese MA, Huang PL, Sawa A, Luo X, Musicki B, Snyder SH, Burnett AL.** Alternatively spliced neuronal nitric oxide synthase mediates penile erection. *Proc Natl Acad Sci USA* 103: 3440–3443, 2006.
10. **Jonakait GM, Gintzler AR, Gershon MD.** Isolation of axonal varicosities (autonomic varicosities) from the enteric nervous system. *J Neurochem* 32: 1387–1400, 1979.
11. **Kiss JP, Vizi ES.** Nitric oxide: a novel link between synaptic and nonsynaptic transmission. *Trends Neurosci* 24: 211–215, 2001.
12. **Klatt P, Schmidt K, Lehner D, Glatter O, Bachinger HP, Mayer B.** Structural analysis of porcine brain nitric oxide synthase reveals a role for tetrahydrobiopterin and L-arginine in the formation of an SDS-resistant dimer. *EMBO J* 14: 3687–3695, 1995.
13. **Leikert JF, Rathel TR, Muller C, Vollmar AM, Dirsch VM.** Reliable in vitro measurement of nitric oxide released from endothelial cells using low concentrations of the fluorescent probe 4,5-diaminofluorescein. *FEBS Lett* 506: 131–134, 2001.
14. **Lin CS, Lau A, Bakircioglu E, Tu R, Wu F, Week S, Nunes L, Lue TF.** Analysis of neuronal nitric oxide synthase isoform expression and identification of human nNOS-mu. *Biochem Biophys Res Commun* 253: 388–394, 1998.
15. **Mashimo H, He XD, Huang PL, Fishman MC, Goyal RK.** Neuronal constitutive nitric oxide synthase is involved in murine enteric inhibitory neurotransmission. *J Clin Invest* 98: 8–13, 1996.
16. **Mashimo H, Kjellin A, Goyal RK.** Gastric stasis in neuronal nitric oxide synthase-deficient knockout mice. *Gastroenterology* 119: 766–773, 2000.
17. **Panda K, Adak S, Aulak KS, Santolini J, McDonald JF, Stuehr DJ.** Distinct influence of N-terminal elements on neuronal nitric-oxide synthase structure and catalysis. *J Biol Chem* 278: 37122–37131, 2003.
18. **Panda K, Ghosh S, Stuehr DJ.** Calmodulin activates intersubunit electron transfer in the neuronal nitric-oxide synthase dimer. *J Biol Chem* 276: 23349–23356, 2001.
19. **Rameau GA, Chiu LY, Ziff EB.** Bidirectional regulation of neuronal nitric-oxide synthase phosphorylation at serine 847 by the N-methyl-D-aspartate receptor. *J Biol Chem* 279: 14307–14314, 2004.
20. **Rao YM, Watanabe Y, Goyal RK.** Identification of pools of calmodulin bound and calmodulin lacking forms of nNOS in the nerve terminals of gut (Abstract). *Gastroenterology* 128: A611, 2005.
21. **Rizzoli SO, Betz WJ.** Synaptic vesicle pools. *Nat Rev Neurosci* 6: 57–69, 2005.
22. **Saur D, Neuhuber WL, Gengenbach B, Huber A, Schusdziarra V, Allescher HD.** Site-specific gene expression of nNOS variants in distinct functional regions of rat gastrointestinal tract. *Am J Physiol Gastrointest Liver Physiol* 282: G349–G358, 2002.
23. **Saur D, Paehge H, Schusdziarra V, Allescher HD.** Distinct expression of splice variants of neuronal nitric oxide synthase in the human gastrointestinal tract. *Gastroenterology* 118: 849–858, 2000.
24. **Su Z, Blazing MA, Fan D, George SE.** The calmodulin-nitric oxide synthase interaction. Critical role of the calmodulin latch domain in enzyme activation. *J Biol Chem* 270: 29117–29122, 1995.
25. **Van Geldre LA, Lefebvre RA.** Interaction of NO and VIP in gastrointestinal smooth muscle relaxation. *Curr Pharm Des* 10: 2483–2497, 2004.
26. **Watkins CC, Sawa A, Jaffrey S, Blackshaw S, Barrow RK, Snyder SH, Ferris CD.** Insulin restores neuronal nitric oxide synthase expression and function that is lost in diabetic gastropathy. *J Clin Invest* 106: 373–384, 2000.
27. **White TD, Leslie RA.** Depolarization-induced release of adenosine 5′-triphosphate from isolated varicosities derived from the myenteric plexus of the guinea pig small intestine. *J Neurosci* 2: 206–215, 1982.